Search for periodicities in the experimental solar neutrino data: A wavelet approach

Gioacchino Ranucci*
Istituto Nazionale di Fisica Nucleare, Via Celoria 16, 20133 Milan, Italy

Stefano Sello†
Mathematical and Physical Models–Enel Research, Via Andrea Pisano 120, 56122 Pisa, Italy
(Received 18 December 2006; published 17 April 2007)

The time series of the ^{8}B solar neutrino measurements released by the Super- Kamiokande and SNO Collaborations have been recently investigated by several groups for possible modulation signatures through standard Fourier-based techniques. In this work we present an alternative analysis of the same data sets based on the wavelet approach, whose key advantage with respect to the traditional methodologies is the ability to capture and follow the time evolution of transient modulation features as well. Moreover, we show the results of the wavelet analysis applied to the mean solar magnetic field and flare index data recorded in the same data-taking period of the two experiments, with the goal of carrying out a direct check of the concurrent presence (if any) of evidence for corresponding time variations in the solar data and in the solar neutrino series. The main outcomes of this investigation are, on one hand, the clear identification of the expected annual modulation variation due to the eccentricity of the Earth's orbit, and on the other, the demonstration that no further reliable time variation signals can be unraveled, within the current experimental sensitivity, in the measured solar neutrino flux.

DOI: 10.1103/PhysRevD.75.073011 PACS numbers: 14.60.Pq, 26.65.+t, 96.60.Jw, 95.75.Wx

I. INTRODUCTION

The results of the two water Cerenkov detectors Super-Kamiokande [1] and SNO [2] provide the firm basis upon which our current understanding of the solar neutrino issue rests. The matter-enhanced oscillation scenario [3,4] delineated by the data from these detectors is further supported by the measurements of the KamLAND reactor neutrino experiment [5]: altogether the experimental results, including also the data from the radiochemical experiments Homestake [6], Sage [7], and Gallex-GNO [8], single out a well-defined large mixing angle (LMA) region in the δm^2_{21}, $\sin^2\theta_{21}$ plane around the best fit values, which are, respectively, 0.312 and 7.92×10^{-5} eV^2 (see for example [9]). These findings essentially close the discovery phase of the long-standing solar neutrino saga, while opening the way to a new chapter of this exciting adventure: the direct exploration with real-time experiments of the sub-MeV sector (up to now investigated only by the radiochemical experiments) with the specific purpose to provide in a short term the direct, real-time measurement of the ^{7}Be component (Borexino and KamLAND solar phase [10,11]) and, if the challenging backgrounds can be overcome, as now appears possible, also of the *pep* line [12].

While the community has been awaiting the new inputs from Borexino and KamLAND, an issue that has recently drawn significant attention in the field is the possible presence of subleading effects accompanying the dominant LMA scenario, mainly the possibility that a sizable neutrino magnetic moment, coupled to rotating variable solar magnetic fields, could induce solar neutrino transition into other flavors via a resonant spin flavor precession mechanism [13–15].

Such a scenario can be probed with the existing experimental results through an accurate search for time modulation signatures in the ^{8}B neutrino time series of the SNO and Super-Kamiokande results. The subject has recently gained much attention, as witnessed by the number of analyses published both by the two collaborations as well as by independent groups. In particular, investigations of the SNO results published in [16,17], performed with similar likelihood and Lomb-Scargle based methodologies, led to the conclusion that no modulation signatures are embedded in the Sudbury data. On the other hand, in [18] a number of potential modulation periods have been claimed in the same data set.

The Super-Kamiokande data have undergone, since their release, a careful scrutiny for periodicities in the different bin formats in which they have been published (5- and 10 day binning), with contradictory results from several groups [19–21] that exploited Lomb-Scargle and likelihood (or χ^2) methodologies. In particular, [21] has shown that the principal sources of these discrepancies are differing treatments of the errors published by the Super-Kamiokande collaboration and the inadequacy of the standard analyses, which focus only on the highest spectral peak, ignoring in the significance assessment other prominent lines present in the spectrum.

Because periodicities hidden by the noise affecting the time-series data would appear as sharp peaks in the power spectrum of the series, all the methods used in the above mentioned analyses produce as a bottom line an estimate of this spectrum. The difficulty associated with this method-

*Electronic address: gioacchino.ranucci@mi.infn.it
†Electronic address: stefano.sello@enel.it

ology is that noise can also produce random peaks in the spectrum; these can attain very great amplitudes, thus hampering the capability of properly detecting actual modulations embedded in the series. The important point of the analysis is thus the significance assessment of the peaks found in the estimated spectrum: this significance is defined as the probability that a peak at least as high as the highest peak found in the actual spectrum could be generated by chance noise fluctuations.

The controversy over the results of the periodicity searches mentioned above suggests that more light could be shed on this intriguing puzzle by exploiting an alternative methodology. For this purpose, the wavelet technique, a powerful generalization of the family of Fourier-based approaches, seems an attractive and interesting possibility for an alternative analysis of the data sets already analyzed with more standard techniques. The purpose of this work is, indeed, to show the results of the application of wavelet analysis to both the Super-Kamiokande and SNO ^{8}B time series; moreover, the results of wavelet analysis applied to the solar magnetic field and flare index data recorded in the same data-taking period of the two experiments are presented, in order to perform a direct check of the concurrent presence (if any) of the same modulation signatures in the solar data and in the solar neutrino series.

II. WAVELET ANALYSIS

Since the introduction of the wavelet transform by Grossmann and Morlet [22], in order to overcome the window limitations of the Gabor transform to multiscale and nonstationary signals, this technique has been extensively applied in a wide range of time series, including many astrophysical analyses such as the study of solar and stellar activity cycles [23–26]. With a local decomposition of a multiscale signal, wavelet analysis is able to properly detect time evolutions of the frequency distribution. This is particularly important when we consider intermittent and, more generally, nonstationary processes. More precisely, the continuous wavelet transform represents an optimal localized decomposition of a real, finite energy, time series, $x(t) \in L^2(\Re)$, as a function of both time, t, and frequency (scale), a, from a convolution integral:

$$(W_\psi x)(a,\tau) = \frac{1}{\sqrt{a}} \int_{-\infty}^{+\infty} dt x(t) \psi^*\left(\frac{t-\tau}{a}\right) \qquad (1)$$

where ψ is called an analyzing wavelet if it verifies an admissibility condition:

$$c_\psi = \int_0^{+\infty} d\omega \omega^{-1} |\hat{\psi}(\omega)|^2 < \infty \qquad (2)$$

with:

$$\hat{\psi}(\omega) = \int_{-\infty}^{+\infty} dt \psi(t) e^{-i\omega t}. \qquad (3)$$

This last condition imposes $\hat{\psi}(0) = 0$, i.e., the wavelet has a zero mean. In Eq. (1) $a, \tau \in \Re$, $(a \neq 0)$ are the scale and translation parameters, respectively [27,28]. In fact, it follows from Eq. (2) that the effectiveness of the wavelet analysis depends on a suitable choice of the analyzing wavelet for the signal of interest. For our time-series application, where we are mainly interested in tracking the temporal evolution of both the amplitude and phase of solar activity signals, we chose to use the family of complex analyzing wavelets consisting of a plane wave modulated by a Gaussian, called Morlet wavelets [29]:

$$\psi(\eta) = \pi^{-1/4} e^{i\omega_0 \eta} e^{-\eta^2/2\sigma^2} \qquad (4)$$

where $\eta = \frac{t-\tau}{a}$, and ω_0 is a nondimensional frequency. σ is an adjustable parameter that can be tuned in order to obtain the optimal wavelet resolution level both in time and frequency, for the characteristic time-scale of the original series [30]. The limited frequency resolution imposes a half-power bandwidth of our wavelet given by $\frac{\Delta f}{f} \approx 0.12$. The local wavelet power spectrum that can be obtained from Eq. (1) is

$$P(k,t) = \frac{1}{2 c_\psi k_0} \left| W\left(\frac{k_0}{k}, t\right) \right|^2, \qquad k \geq 0 \qquad (5)$$

at frequency k and time t; it is generally visualized by proper contour maps.

Following Foster (1996), here we consider an extension of the above wavelet formalism in order to handle irregularly sampled time series correctly. The wavelet transform is viewed as a suitably weighted projection onto three trial functions giving the Weighted Wavelet Z transform and the Weighted Wavelet Amplitudes. For all the mathematical details of this formulation and its applications we refer to the Foster (1996) paper [31]. Many applications of the wavelet analysis have suffered from an apparent lack of quantitative evaluations, especially by the use of arbitrary normalization, and the lack of a statistical significance test in order to estimate the reliability of results. Here we used power spectrum normalization and significance levels following the approach suggested by Torrence *et al.* (1997) [29]. We first assume an appropriate background spectrum, and we suppose that different realizations of the considered physical process will be randomly distributed about this expected background spectrum. The actual spectrum is compared against this random distribution. In the present work we take as the background spectrum a red noise spectrum modeled through a univariate lag-1 autoregressive process:

$$x_n = \alpha_{x_{n-1}} + z_n \qquad (6)$$

where z_n is derived from a Gaussian white noise and α is the lag-1 autocorrelation, here estimated by

$$\alpha = \frac{\alpha_1 + \sqrt{\alpha_2}}{2} \qquad (7)$$

where α_1 and α_2 are, respectively, the lag-1 and lag-2 autocorrelations of the considered time series. The discrete normalized Fourier power spectrum of this red noise is

$$P_k = \frac{1-\alpha^2}{1+\alpha^2-2\alpha\cos(\frac{2\pi k}{N})} \quad (8)$$

and the following null hypothesis is defined for the wavelet power spectrum: we assume the red noise spectrum to be the mean power spectrum of the time series; if a peak in the wavelet power spectrum is significantly above this background spectrum (here at 95% or 99% confidence level), then it can be considered an interesting candidate as a real feature of the time series, thus deserving further investigation [29].

In this work, we show some results of the wavelet analysis applied to different solar neutrino fluxes in order to characterize the time evolution properties of some characteristic frequencies already detected and well documented in the literature. The local properties in time of these periodicities can allow a better interpretation of their origin and a correlation of the neutrino flux with some basic solar cycle properties, such as the periodic emergence of intense magnetic flux or the time modulation of the solar mean magnetic field.

III. CHARACTERISTICS OF THE DATA

A. Description of the SNO data sets

It is well known that the SNO detector is a heavy water Cerenkov detector that measures ^{8}B solar neutrinos via charged-current and neutral-current interactions on deuterons in 1 kton of D_2O, and also through neutrino-electron elastic scattering interactions [2]. The data sets used in this analysis, officially released by the SNO collaboration, are similar to those used in the periodicity search reported in [16]. They are related to the two first phases of the experiment, i.e., the pure D_2O phase and the salt phase, in which salt has been added to the heavy water in order to increase the neutron detection efficiency.

The data-taking period started on November 2, 1999 and encompassed in total about 1400 calendar days. For both phases, the SNO collaboration released two files, one with the number of daily detected events, and the other with the specification of the runtime periods during each day of data taking. A proper periodicity analysis clearly has to take into account the actual live time within each day of data taking in order to normalize the detected counts properly.

It must be pointed out that there is a difference between the released data and those used by the SNO Collaboration in its periodicity search: while the latter retain the full time information, the former are characterized by the rounding of the time of each event to the units of day. Practically, this implies that the data have been published in the format of 1 day binning.

The event rates vs time, obtained through a suitable bin manipulation similar to that used in [16], are displayed in Figs. 1 and 2 for the D_2O and salt phases, respectively. In particular, some of the nominal 1 day bins have been merged together when their individual widths were much shorter than the nominal value, in order to avoid large scattering in the data display.

The overall rate is 9.35 eV/day in the case of the D_2O phase, and 11.85 eV/day in the case of the salt phase. The fact that the shapes of the two figures reproduce well the details of the two corresponding figures in [16] gives confidence that the retrieval and arrangement of the data have been done properly. In particular, each point of the series in the two figures is characterized by a time value which is the weighted mean time of the corresponding bin, evaluated so as to take into account properly the bin live time, and by a corresponding ordinate value which is the

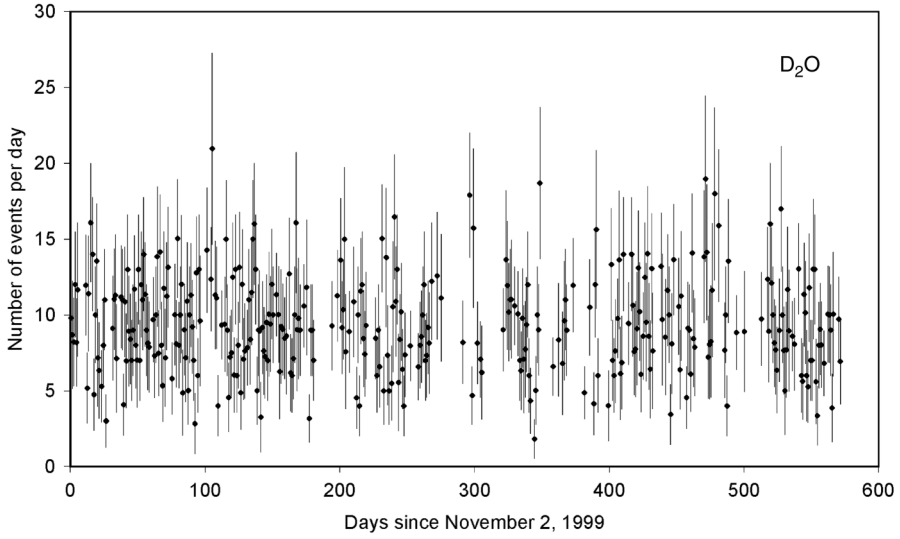

FIG. 1. The event rates vs time for the SNO D_2O phase.

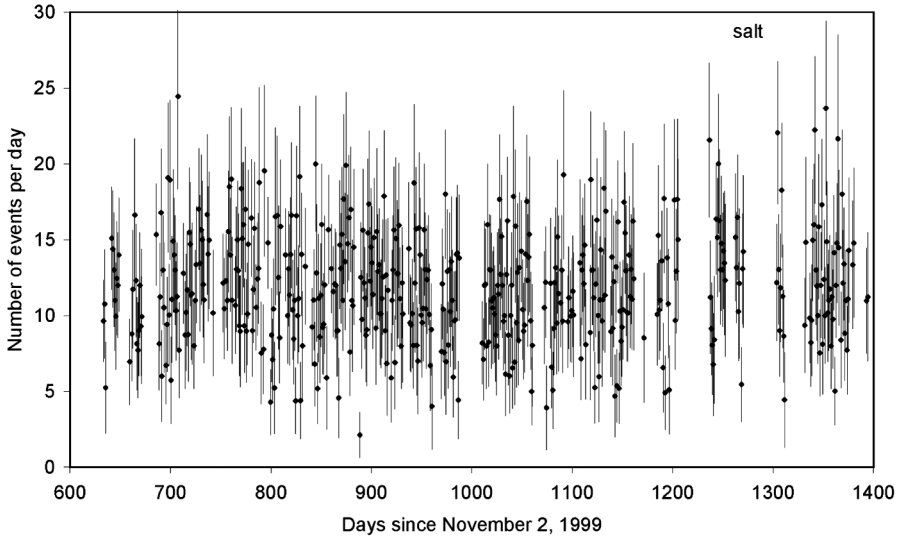

FIG. 2. The event rates vs time for the SNO salt phase.

normalized count rate in the same bin, i.e., the total counts in that bin divided by the corresponding live time. This summary description of the data is enough for the purpose of the present analysis. For further details on the characteristics of the data sets the reader can refer to [16].

B. Description of the Super-Kamiokande data sets

The Super-Kamiokande detector is a 50 kton water Cerenkov detector, in which neutrinos are detected only through neutrino-electron elastic scattering interactions [1]. The data set used in the present analysis is that related to the Super-Kamiokande I phase, encompassing more than five years, from May 1996 to July 2001.

It should be pointed out that, while the data published by SNO represent the actual sequence of detected events (with the only limitation being the above mentioned truncation to 1 day unit), the data released by Super-Kamiokande are already converted to neutrino fluxes, expressed in units of 10^6 cm^{-2} s^{-1}, and binned, either in 10- or 5 day bins. For each bin, as well as this flux value, the following data were also provided: the respective mean live time t_{wk}, properly evaluated in order to take into account the live time of the detector; and the relevant correction factor to remove the 7% peak-to-peak annual variation due to the eccentricity of the Earth's orbit around the Sun. However, in all the calculations reported in the following, we have preferred not to apply such a correction, in order to leave the data fully intact.

Also, for each 10- or 5 day long segment, the start time t_{sk}, the end time t_{ek}, and the two asymmetric errors σ_k^{up} and σ_k^{down} are given in the data sets. The sequence of the data

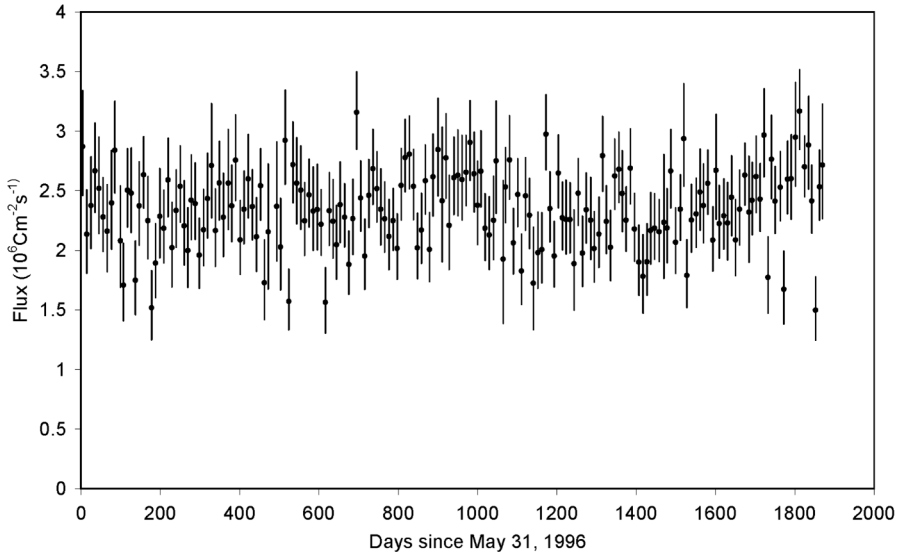

FIG. 3. Super-Kamiokande data set for the 10-day bin case.

for the 10 day bin case is plotted in Fig. 3. For more details, the interested reader can refer directly to [19]. In the following, the analysis will be focused mainly on the more sensitive 5 day bin data set, though some results concerning the 10 day binned data set will be reported, too.

IV. RESULTS OF THE SOLAR NEUTRINO DATA WAVELET ANALYSIS

A. Super-Kamiokande data

The principal information derived from the application of the wavelet formalism to real data is the local spectrum, Eq. (5), which allows us to resolve the time evolution of the related frequency distribution. The physical significance of a given frequency peak is then strictly correlated to its time persistence, as well evidenced by the wavelet analysis. This concept will be clearly illustrated in the following description of the results obtained on the 5- and 10-day binned data sets of the Super-Kamiokande I experiment.

1. 5-day binned data

In Fig. 4 we show the results of the wavelet analysis applied to the Super-Kamiokande 5-day binned data, covering the time interval May 31, 1996–July 15, 2001. The upper panel shows the original time series in its natural units (red line); time is expressed in years. The central panel shows the amplitudes of the wavelet local power spectrum in terms of a color contour map. White lines correspond to the strongest local energetic contributions to the power spectrum (wavelet ridge). The horizontal time axis corresponds to the axis of the upper time series, and the vertical scale axis is the period expressed in years. Thus the analyzed period range spans from 7.3 days (i.e. 0.02 yr^{-1}) to 5.1 years.

The right panel shows the mean wavelet spectrum (an averaged and weighted Fourier spectrum) obtained through a time integration of the local map. The significance of the power was tested using an adjustable red-noise autoregressive lag-1 background spectrum both at 95% (green line) and 99% (blue line) confidence levels, according to the methodology developed in [29,32]. An evident feature of the wavelet local power map of the 5-day binned SK data is, for a large portion of the map itself, the discontinuity of its time distribution; i.e., the periodicity content is highly intermittent showing peaks strongly localized in time. The red-noise lag-1 autocorrelation coefficient is 0.079. The local Nyquist limit, dictated by the binning of the data, is located around 0.027 yr; thus the results of the analysis above such a limit are to be taken with some caution. They are reported here only for the purpose of comparison with previous studies, which also extended up to the period of 0.02 years.

In the map some of the main local contributions are indicated. From the mean wavelength spectrum, we infer that the two most significant spectral contributions below the 0.027 yr Nyquist limit are located at the periods of 2.8 years and 1.1 years, both exceeding the 95% CL limit (even though remaining below the 99% CL value). The local map clearly indicates the persistency of these two lines over almost the entire data-taking period; this behavior is as expected for the line tagged at 1.1 yr, which obviously corresponds to the annual modulation of the

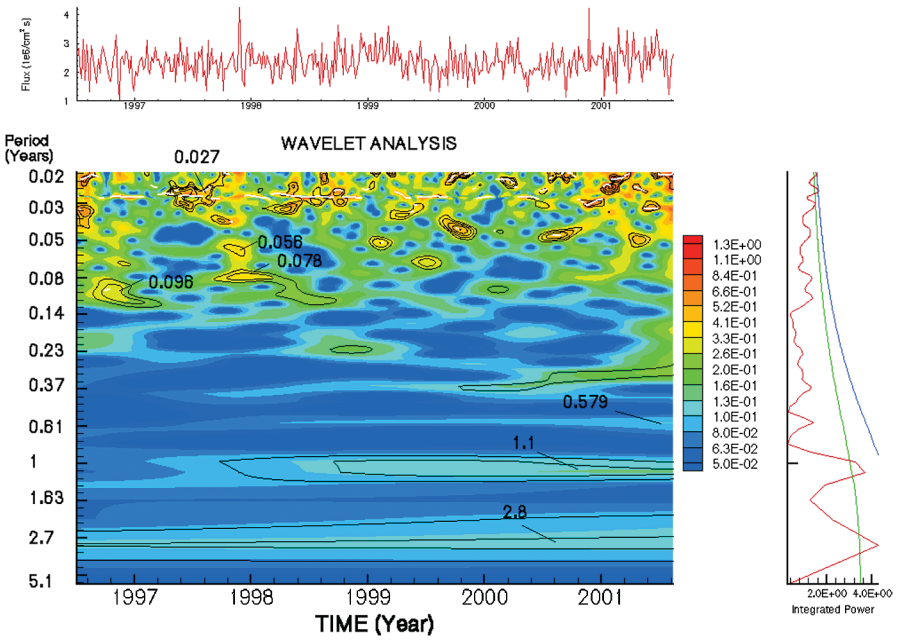

FIG. 4 (color). Local wavelet map of the 5-day binned Super-Kamiokande I data.

flux due to Earth's orbital eccentricity around the Sun (slightly shifted with respect to the nominal value).

Three other lines emerging in the mean wavelength spectrum below the Nyquist limit are located at the periods of 0.1 yr, 0.082 yr, and 0.05 yr, but none of them reach even the 95% CL. The first two lines correspond to the islands in the local map identified at the local periods 0.098 yr and 0.078 yr, while the third is the collective result of the island identified at 0.056 yr plus the other four islands essentially aligned with it on its right side.

While passing to the region above the Nyquist limit, with the caveat mentioned previously, the first thing to note is that the wavelet ridge is very close to the Nyquist limit itself. Above this limit, the mean wavelength spectrum features two lines with high significance at periods, respectively, 0.031 yr and 0.025 yr. The former touches the 95% CL, while the latter reaches the 99% value. It should be noted, in particular, in the local map, that the island marked at 0.027 makes a strong local contribution to the 0.025 yr line. Finally, the mean wavelength spectrum approaches the 0.02 yr upper limit of the spanned frequency range with a further rise, reflecting with this behavior the presence of many fragments of the wavelet ridge close to the 0.02 yr period itself. We will discuss in Sec. VI how these results compare with previous analyses of the same data set and with the outcomes of the studies of the solar magnetic field evolution over the same period.

2. 10-day binned data

In Fig. 5 we show the wavelet analysis of the 10-day binned flux data. The red-noise lag-1 autocorrelation coefficient is 0.072. In the present case the local Nyquist limit is located at the period of about 0.057 yr.

It can be noted that both the map and the integrated power faithfully reproduce the same quantities evaluated for the 5-day bin data in the region of the long periodicities, up to the period of 0.14 yr;, in particular, the 1.1 yr and 2.4 yr periodicities are the counterparts of the long-term features found in the 5-day binned data set, even if for the latter there is a certain shift. Also from the period of 0.14 yr up to the Nyquist limit of 0.057 yr there is a correspondence with the 5-day map, in the sense that the three islands at 0.098, 0.078, and 0.056 present there appear also in the 10 day map.

It is interesting and instructive to note that the shape of the third island appears in the 10-day map to be distorted by the alias effect: since this island touches the Nyquist limit, it is accompanied by its companion image, specularly reflected around the Nyquist limit itself.

In the integrated power the two 5-day lines at 0.1 and 0.082 years are still present, but (and this is the major difference) with the former reaching a significance as high as the 99% CL. Despite this high significance in the integrated power, the local wavelet map shows that such a component features a very peculiar time evolution: it is extremely strong in the first data-taking period and then appears only intermittently and more weakly up to the end of the data acquisition. Examining the same line in the 5-day map, we trace back there a very similar time behavior. Above the Nyquist limit, we note the very strong line at 0.037 (which, as other authors have already pointed out, is in alias relationship with the 0.1 line) and that at 0.022, which seems to be the counterpart of the 0.025 line in the 5-day analysis.

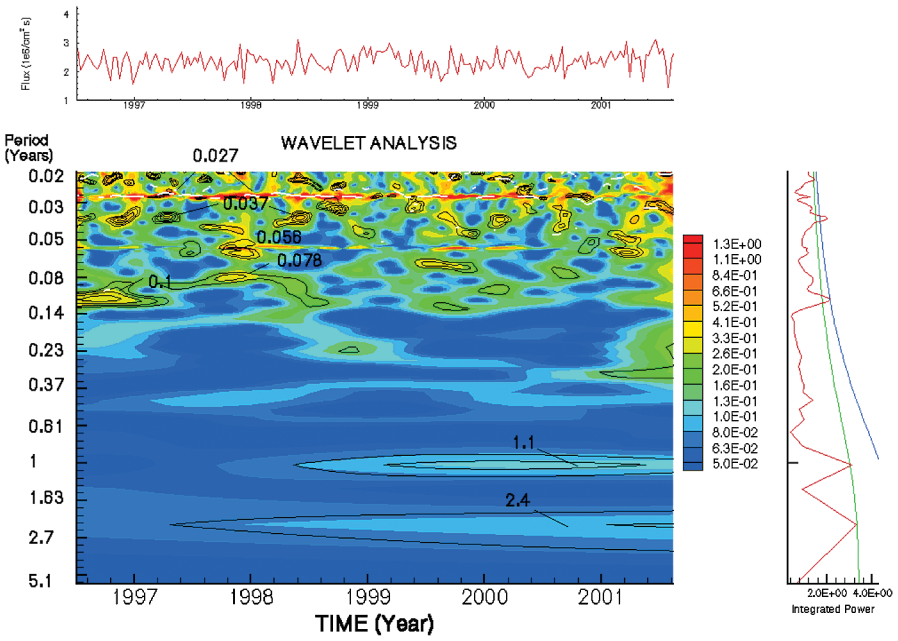

FIG. 5 (color). Local wavelet map of the 10-day binned Super-Kamiokande I data.

It should also be outlined that most of the wavelet ridge is located at 0.027, as in the 5-day case. So, in summary, the analysis of the 10 day binned data set reproduces the main features already detected in the 5 day binned time series, with the exception that the line at 0.1 appears with a much higher significance. Further discussions of these results are postponed to Sec. VI.

B. SNO data

In this subsection we analyze the data released by the SNO collaboration. The relevant maps are plotted in the same range used for the SK analysis, even though the Nyquist limit is now much higher and thus, in principle, the analysis could be extended well beyond the period of 0.02 yr. Figure 6 shows the wavelet analysis result of the D_2O phase covering the time interval from November, 2, 1999 to May, 27, 2001 and which partially overlaps (30%) the Super-Kamiokande data. The red-noise lag-1 autocorrelation coefficient is 0.11. Note that the 1-day flux data unit here is the events count number.

Considering the highest peaks detected through the wavelet ridge, we can note the absence of stable modulations (there is, indeed, a high level of fragmentation), which is reflected in the integrated power by lines that all remain below the 95% CL value.

The expected annual modulation appears with the correct frequency localization, but with low significance, well below the 95% level. An explanation for this peculiarity could be, besides the limited time interval spanned by the data, the larger statistical errors for the SNO data with respect to those of SK.

Considering the salt phase, covering the time interval July 25, 2001–August 27, 2003, the wavelet analysis confirms the intermittent structure of the main short-term peaks, with some evidence for the 0.027 yr and 0.056 yr periods, though they barely arrive at the 95% level (see Fig. 7). The red noise lag-1 autocorrelation coefficient is 0.11.

A puzzling peculiarity of this second data set is the presence of a highly significant low frequency line (in the local wavelet map it appears to persist over the whole data-taking period). Presumably it is the annual modulation line, but it is not clear why its position is so shifted with respect to its nominal frequency.

As a further check of the data, we repeated the analysis of SNO D_2O and salt phases up to the Nyquist limit (mean value: 108 yr^{-1}). We verified that in this extended range, the wavelet calculation shows only evidence of a significant, though intermittent, frequency feature near 66 yr^{-1} (or 5.5 days) in the former data set, not present in the latter. Thus, globally, even from 0.02 yr up to the Nyquist limit,

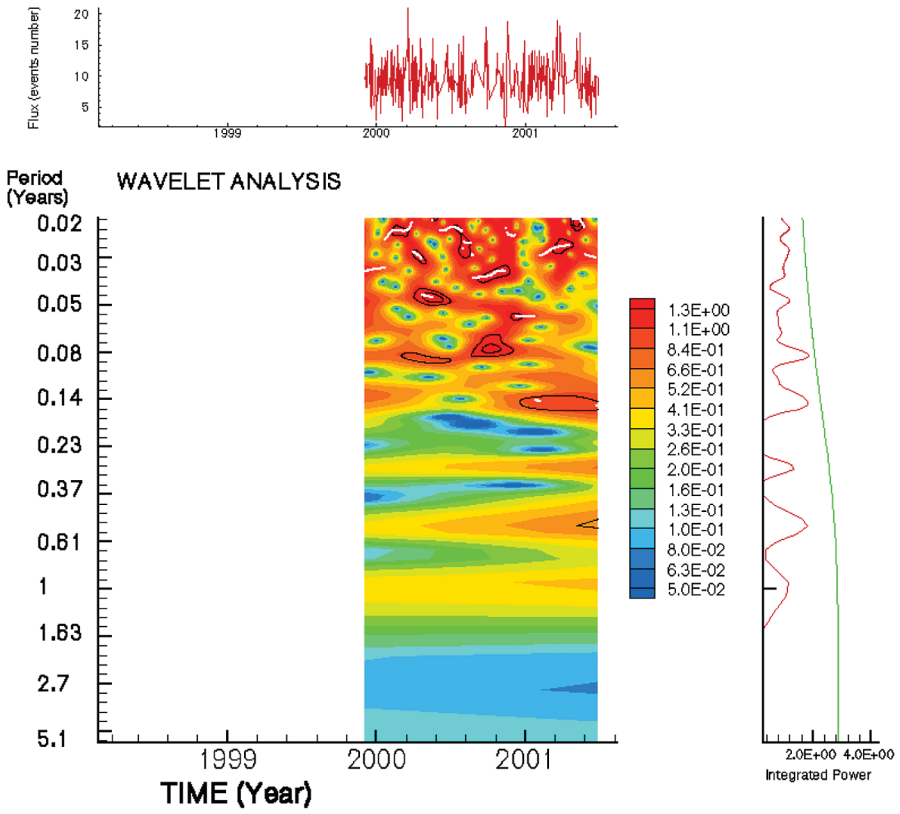

FIG. 6 (color). Local wavelet map of the SNO D_2O phase.

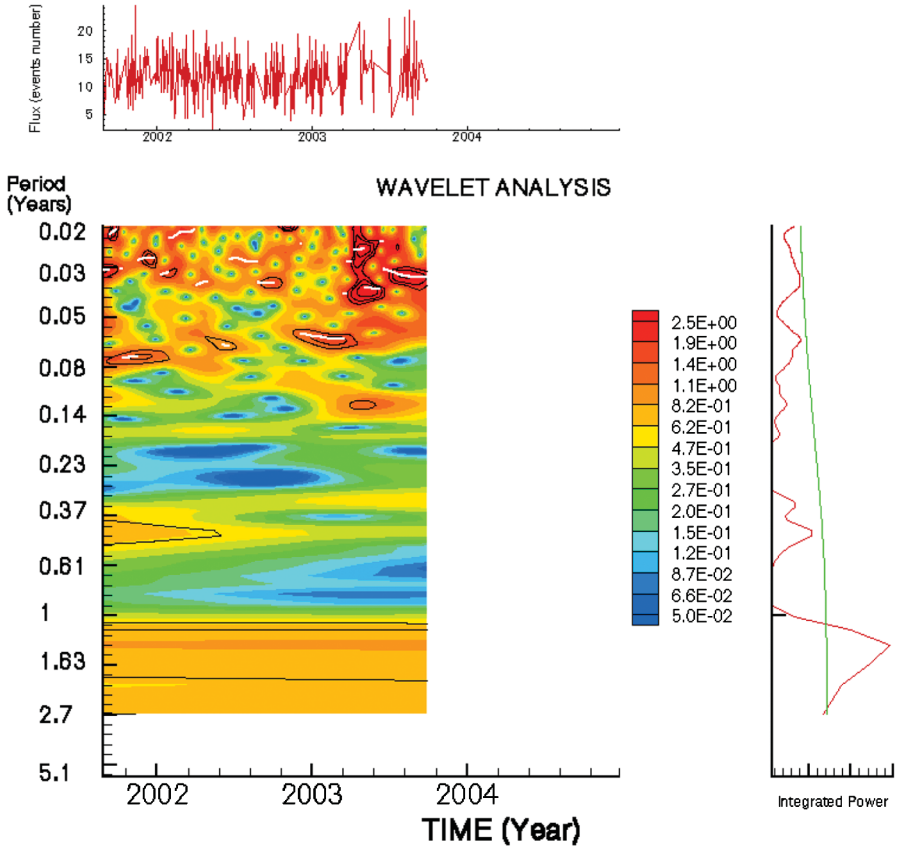

FIG. 7 (color). Local wavelet map of the SNO salt phase.

the wavelet analysis does not provide evidence for persistent, significant spectral features.

V. ANALYSIS OF THE SOLAR ACTIVITY DATA

In order to perform a cross analysis between the solar neutrino data and the solar magnetic field time behavior, we performed a wavelet analysis of the spatially averaged solar magnetic field and of the flare index data recorded in the corresponding time interval. The first set of data allows us to check possible interaction mechanisms between the neutrino flux and the global magnetic field evolution during different phases of the solar magnetic cycle; the second set of data permits us to verify the possible role of strong, local magnetic fields related to very intense solar active regions in influencing the neutrino flux.

The daily mean magnetic field data were obtained via the web site of the Wilcox Solar Observatory (courtesy of J. T. Hoeksema) [33]; the corresponding wavelet analysis results are shown in Fig. 8. The magnetic field data are in microTesla and cover the same time interval as the Super-Kamiokande data (and hence overlap also the D_2O phase of the SNO experiment). The prominent stable peaks are located, as expected, near 0.038 yr and 0.078 yr and are related to the solar rotation rates. Beside these, there are no other peaks with significances that could draw some attention.

The second solar data used in this study, the daily solar flare activity data, were calculated by T. Atac and A. Ozguc from Bogazici University, of the Kandilli Observatory of Instabul [34] (Fig. 9). As is well known, in the solar flare processes there are some significant localized peaks, which during the more active phase of the current solar cycle (cycle number 23) are mainly those located at the periods 0.027 yr, 0.057 yr, 0.097 yr, 0.33 yr, and 0.71 yr. Clearly the structure of the wavelet map in this case is more intermittent than that of the previous map, reflecting the localized nature of the flare phenomenon; this is why, in the mean wavelet spectrum, the main spectral components do not exhibit very strong significances. In the next section, the solar activity data and the neutrino data will be considered together to perform a global cross-check.

VI. DISCUSSION AND COMPARISON WITH PREVIOUS RESULTS

A. 9.42–9.43 yr^{-1} component

Most of the current interest in the careful scrutiny of the available solar neutrino data for possible time modulations is motivated by some evidence in the first analyses carried out on the Super-Kamiokande I data set [19–21] for a line with frequency 9.42–9.43 yr^{-1} (i.e. a period of about 0.11 yr), but for which the statistical significance is con-

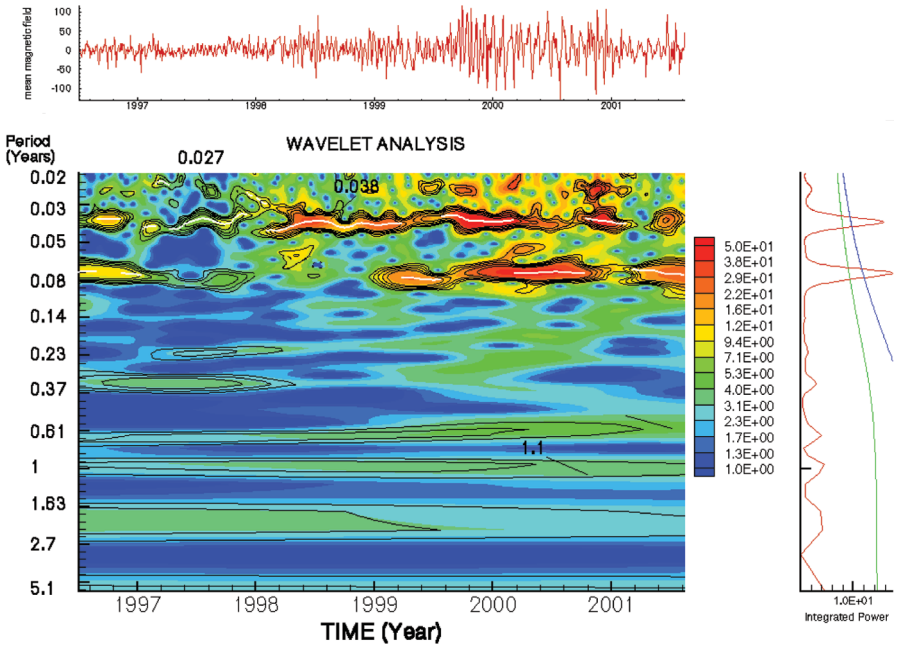

FIG. 8 (color). Local wavelet map of the daily solar mean magnetic field.

troversial. The studies carried out afterwards on the SNO data sets [16,17] pointed out that such a line was not present there, relegating it to the condition of a peculiar feature only of the SK data, and hence very likely unconnected with intrinsic properties of the underlying neutrino flux.

The present wavelet analysis not only reproduces these outcomes (therefore confirming the expected consistency between the standard spectral analysis and the wavelet methodology), but allows us to shed more light on the characteristics of this line in the SK data. In particular, we can draw the conclusion that such a line features, in both the 5- and 10 day data set, the same intermittent time evolution, with the preponderant contribution represented by a localized episode at the beginning of the data taking, in 1996, followed later on by some weak episodes. The higher statistical significance in the 10 day data set is linked to the higher local power featured by the initial episode with respect to the 5 day case.

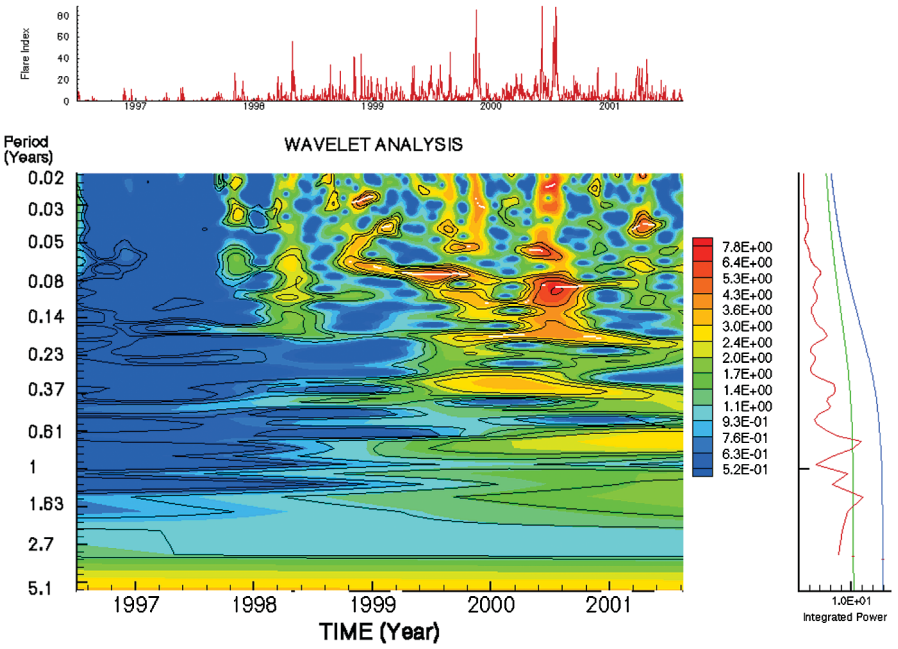

FIG. 9 (color). Local wavelet map of the daily solar flares activity data.

The wavelet analysis also confirms the alias interpretation of the 0.037 strong line in the 10 day spectrum [20,21], which indeed disappears in the 5-day result. Furthermore, in the SNO data, both in the salt phase and in the D_2O phase, there is no hint whatsoever of a possible spectral component around this frequency.

However, the wavelet analysis indicates that the comparison with SNO data alone is not fully conclusive to wipe out the evidence stemming from the episode of the beginning of the SK period, since at that time SNO was not yet in operation. On the other hand, the comparison with the solar data points out that in the same period, there is no solar activity that could justify (via the hypothetical magnetic moment coupling referred at the beginning of this paper) even a local time variation of the solar neutrino flux.

In conclusion, the concurrent analyses of the various solar and neutrino data sets taken into account demonstrate that the 9.42–9.43 yr^{-1} component is likely to be only a peculiar feature of the SK data, with no connection to the underlying neutrino flux.

B. Long periodicities

Probably the most interesting result of the wavelet analysis is the unambiguous identification of the annual modulation spectral component in the SK data, captured with a significance above the 95% limit, which can be considered as a nice, further proof of the solar origin of the SK measured data. Unfortunately a similar crystal clear result is not obtained for the SNO data, for in the D_2O data set the annual line is detected, but with low significance, while in the salt data there is a highly significant line, almost surely just the annual line, but not located at the correct frequency.

Moreover, in the SK data a line with period 2.8 yr is present, featuring significance and persistence similar to those of the annual modulation line. Interestingly, this line was also detected through the Ferraz-Mello method in studies reported in [35,36] (in [36], the high significance detection of the annual line was also reported). By examining the other maps we see, however, that such a line does not have any counterpart in the solar activity data and in the SNO data; thus it seems very hard to attribute this feature to the neutrino flux.

C. Short periodicities

The analysis of the 5-day SK data set reported in [20,21], in addition to the 9.42–9.43 yr^{-1} frequency line, gave evidence of some high frequency lines in the range between the Nyquist limit and the 0.02 yr (50 yr^{-1}) upper limit of the analysis range. These lines have counterparts in the wavelet analysis in the short-period features shown both by the local map and by the mean integrated spectrum, especially while considering the 5 day SK data set, thus demonstrating again that the wavelet analysis produces results consistent with those stemming from the more standard Lomb-Scargle-like methodologies. Again, these features are largely not supported by similar lines in either the SNO data set or in the solar activity maps. Indeed, the only limited association that could be traced is that between two episodes at the period of 0.027 yr, occurring at the time 1997.5, which are present both in the 5-day SK map and in the solar magnetic activity map.

This being the only (even circumscribed and limited) coincidence detected, we conclude that, from the cross-comparison of the wavelet maps of the different data sets analyzed, even in the short-period range there are no common spectral features that could be traced back as manifestations of intrinsic properties of the neutrino flux.

VII. CONCLUSION

The careful comparison of the wavelet analysis of the solar neutrino data from the SNO and Super-Kamiokande experiment with the solar activity parameters proved to be very effective in unraveling the time characteristics of the measured neutrino flux. The main conclusions of the analysis are: (a) the confirmation of the presence of a frequency feature in the SK data consistent with previous analyses which located it at the frequency 9.42–9.43 yr^{-1}; (b) the identification of a well-localized episode at the beginning of the SK data-taking period which is the main origin of that frequency; (c) the demonstration that such a frequency has no counterpart in the other analyzed data, thus cannot be attributed to the underlying neutrino flux; (d) the identification of the annual modulation, which is very clear in the SK data set, though more foggy in the SNO data; (e) the exclusion, through the cross-comparison of all the available data sets, of other potential features both in the long periodicity (2.8 yr) and short periodicity ranges.

Therefore, in summary, the main outcome of the wavelet analysis presented in this work is that in the available solar neutrino data it is not possible to find evidence of modulation signatures pertaining to the measured neutrino flux other than the expected annual line. The current data, hence, do not support the existence of the hypothesized coupling mechanism between the possible neutrino magnetic moment and the solar magnetic fields.

ACKNOWLEDGMENTS

The authors would like to thank the Super-Kamiokande and SNO Collaborations for making their data publicly available.

[1] S. Fukuda *et al.* (Super-Kamiokande Collaboration), Phys. Lett. B **539**, 179 (2002).
[2] S. N. Ahmed *et al.* (SNO Collaboration), Phys. Rev. Lett. **92**, 181301 (2004).
[3] L. Wolfenstein, Phys. Rev. D **17**, 2369 (1978).
[4] S. P. Mikheev and A. Y. Smirnov, Sov. J. Nucl. Phys. **42**, 913 (1985).
[5] K. Eguchi *et al.* (KamLAND Collaboration), Phys. Rev. Lett. **90**, 021802 (2003).
[6] B. T. Cleveland *et al.*, Astrophys. J. **496**, 505 (1998).
[7] J. N. Abdurashitov *et al.* (SAGE Collaboration), Phys. Rev. C **60**, 055801 (1999).
[8] W. Hampel *et al.* (GALLEX Collaboration), Phys. Lett. B **447**, 127 (1999).
[9] G. L. Fogli *et al.*, hep-ph/0608060.
[10] G. Alimonti *et al.* (Borexino Collaboration), Astropart. Phys. **16**, 205 (2002).
[11] T. Mitsui (KamLAND Collaboration), XXII International Conference on Neutrino Physics and Astrophysics, Santa Fe, 2006.
[12] H. Back *et al.* (Borexino Collaboration), hep-ex/0601035.
[13] O. G. Miranda *et al.*, Nucl. Phys. **B595**, 360 (2001).
[14] E. K. Akhmedov and J. Pulido, Phys. Rev. D **66**, 053006 (2002).
[15] B. C. Chauan *et al.*, J. High Energy Phys. 07 (2005) 051.
[16] B. Aharmin *et al.* (SNO Collaboration), Phys. Rev. D **72**, 052010 (2005).
[17] G. Ranucci and M. Rovere, Phys. Rev. D **75**, 013010 (2007).
[18] K. Ghosh and P. Raychaudhuri, hep-ph/0606317.
[19] J. Yoo *et al.* (Super-Kamiokande Collaboration), Phys. Rev. D **68**, 092002 (2003).
[20] P. A. Sturrock *et al.*, Phys. Rev. D **72**, 113004 (2005).
[21] G. Ranucci, Phys. Rev. D **73**, 103003 (2006).
[22] A. Grossmann and J. Morlet, SIAM J. Math. Anal. **15**, 723 (1984).
[23] A. R. Ochadlick, H. N. Kritikos, and R. Giegengack, Geophys. Res. Lett. **20**, 1471 (1993).
[24] J. K. Lawrence, A. C. Cadavid, and A. A. Ruzmaikin, Astrophys. J. **455**, 366 (1995).
[25] P. Frick, S. L. Baliunas, D. Galyagin, D. Sokoloff, and W. Soon, Astrophys. J. **483**, 426 (1997).
[26] R. Oliver, J. L. Ballester, and F. Baudin, Nature (London) **394**, 552 (1998).
[27] I. Daubechies, Ten Lectures on Wavelets, SIAM, Philadelphia, 1992.
[28] Mallat and Stéfane, *A Wavelet Tour of Signal Processing* (Academic Press, San Diego, California, 1998), 2nd ed..
[29] C. Torrence and G. P. Compo, Bull. Am. Meteorol. Soc. **79**, 1, 61 (1998).
[30] W. Soon, P. Frick, and S. Baliunas, Astrophys. J. **510**, 2, L135 (1999).
[31] G. Foster, Time Series Analysis by Projection. I. Statistical Properties of Fourier Analysis (1996), Vol. 111, p. 541.
[32] S. Sello, New Astron. Rev. **8**, 2, 105 (2003).
[33] Wilcox Solar Observatory, http://quake.stanford.edu/wso.
[34] A. Ozguc and T. Atac, Sol. Phys. **123**, 357 (1989).
[35] T. Shirai, Sol. Phys. **222**, 199 (2004).
[36] P. Raychaudhuri, K. Ghosh, and A. S. Mandal, Proceedings of the 29th International Cosmic Ray Conference on Time Variations of the SuperKamiokande Solar Neutrino Flux Data, Pune, India, 2005 (2005), Vol. 9, pp. 115–118.